Journal of Advanced Research in Fluid Mechanics and Thermal Sciences

Journal homepage:
https://semarakilmu.com.my/journals/index.php/fluid_mechanics_thermal_sciences/index
ISSN: 2289-7879

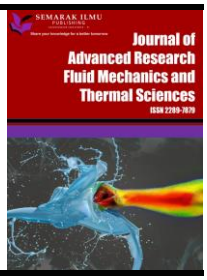

Sustainable Biochar Carbon Microparticles Based on Mangosteen Peel as Biosorbent for Dye Removal: Theoretical Review, Modelling, and Adsorption Isotherm Characteristics

Asep Bayu Dani Nandiyanto[1,2,*], Meli Fiandini[1], Denaya Ayu Fadiah[1], Pitri Aprilia Muktakin[1], Risti Ragadhita[1], Willy Cahya Nugraha[2], Teguh Kurniawan[3], Muhammad Roil Bilad[2,4], Jumril Yunas[5], Abdulkareem Sh. Mahdi Al Obaidi[6]

[1] Fakultas Pendidikan Matematika dan Ilmu Pengetahuan Alam, Universitas Pendidikan Indonesia, Jl. Dr. Setiabudhi no. 229, Bandung 40154, Indonesia
[2] Research Unit for Clean Technology, National Research and Innovation Agency, Jl. Cisitu Sangkuriang, Bandung 40135, Indonesia
[3] Departement of Chemical Engineering, Sultan Ageng Tirtayasa, Cilegon 42435, Banten, Indonesia
[4] Faculty of Integrated Technologies, Universiti Brunei Darussalam, Jalan Tungku Link, Bandar Seri Begawan BE 1410, Brunei Darussalam
[5] Institute of Microengineering and Nanoelectronics, Universiti Kebangsaan Malaysia, Bangi 43600, Selangor, Malaysia
[6] School of Engineering, Taylor's University, Jl. Taylors, Subang Jaya 47500, Selangor, Malaysia

ARTICLE INFO

Article history:
Received 10 December 2022
Received in revised form 18 March 2023
Accepted 24 March 2023
Available online 11 April 2023

Keywords:
Biochar; carbon; isotherm adsorption; mangosteen peel; particle size; Sustainable Development Goals (SDGs)

ABSTRACT

Environmental problems and global energy demand increase every day. The quality of water and sanitation is a very hot topic of discussion. The principles of sustainable development (SDGs) by utilizing renewable materials need to be applied to overcome this problem. One way is through the use of agricultural waste as a renewable carbon material. The study aims to analyze the adsorption characteristics of sustainable carbon microparticles based on mangosteen peel for dye removal. This study also evaluates adsorption isotherms based on its microparticle size effects. In short, carbon preparation was started by mangosteen peel carbonization at 250˚C for 5 hours and tested using sieves (i.e., 125, 250, 500, 1000, and 2000 µm) to obtain a certain size of carbon. Adsorption was evaluated based on a specific particle size using a batch adsorption reactor. Curcumin was used as a model organic dye. The findings showed that particle sizes influence physical adsorption with repulsive interactions between adsorbates. Adsorption in the large particles (i.e. 2000 and 1000 µm) occurs in the multilayer adsorption process with pore filling, while that in the small particles (i.e., 500 µm) occurs in the monolayer adsorption process with pore filling. Small-sized carbon does not provide enough active sites (such as the absence of a pore structure on the surface) for the adsorbate, leading to the creation of a monolayer during adsorption. Meanwhile, in large-sized carbon, the pore-filling mechanism in the adsorbent surface cause the formation of multilayer adsorption. This research is important to understand the application of adsorption using agricultural waste-based adsorbents by observing the phenomena occurring during the adsorption process.

* *Corresponding author.*
E-mail address: nandiyanto@upi.edu

https://doi.org/10.37934/arfmts.105.1.4158

1. Introduction

Environmental problems and global energy demand increase every day, making the quality of water and sanitation becomes a hot topic of discussion. The issues in the global clean water demand increase as the population increases [1,2]. Previous studies have connected these issues to facing various emerging contaminants, such as heavy metal pollution, dyes, pesticides, pharmaceuticals, radioactive elements, and phenol derivative compounds [3-10].

Dyes, which are commonly found in effluents from various industrial sectors, including textiles, food products, tanneries, pulp and paper, paints, and pigments, are one of the most significant groups of pollutants due to their highly toxic nature [11]. Additionally, the presence of dyes in water can cause water to turn colored and limit the amount of dissolved oxygen in the water, which has a negative influence on aquatic life [11]. To guarantee the availability of water, a water treatment system is needed that applies the principles of sustainable development goals (SDGs).

The various methods used for wastewater treatment are classified as follows: traditional methods (such as sedimentation, flocculation, coagulation, filtration, and aeration), physical (such as the ion exchange, adsorption, irradiation, nano, membrane or ultra-filtration, and reverse osmosis), chemical (such as advanced oxidation process and ozonation), and biological (such as anaerobic-aerobic, enzyme degradation, and the adsorption by microbial biomass) [11-16]. However, several of these methods have drawbacks, such as generating hazardous by-products, needing huge processing areas, consuming a lot of energy, or producing an offensive stench [17]. Among various dye removal techniques, adsorption is the procedure of choosing that shows good performance because it can be used to remove various types of dyes from materials [18]. Adsorption has been considered a superior method for water treatment in terms of flexibility, initial cost, simplicity of design, and ease of operation. In addition, adsorption does not result in the production of harmful pollutants [19].

To realize SDGs, the development of materials from renewable materials must be implemented [20]. Realizing that developing materials from renewable resources can result in inexpensive adsorbents and also help to solve the problems with the adsorption method caused by the use of expensive adsorbent materials. Carbon is the material most commonly used in industry because it has the potential to be used as an adsorbent, catalyst, degassing agent, drug delivery system, and storage of energy materials [21]. Moreover, carbon particles have a large surface area and porous structure with high pore volume, as well as stability against chemical and thermal conditions. These unique characteristics make carbon particles ideal for solving environmental problems [22]. Over the past few years, many studies have succeeded in developing renewable carbon as an adsorbent from agricultural wastes, such as rice husk, red dragon, pineapple peel, soursop skin, pumpkin seeds, corn cobs, and papaya seed [23-28]. Agricultural waste-based adsorbent materials (raw or active materials) receive more attention due to their low cost, availability in practically every region of the world, and obtainment by only a few preparation stages with easy synthesis procedures [13]. In addition to the technical aspect, it turns out that agricultural waste possesses holes, a loose structure, and functional groups such as hydroxyl, carboxyl, and others that efficiently aid in dye adsorption [29].

Here, this study aimed to analyze the adsorption characteristics of renewable carbon from mangosteen peel. Ten adsorption isotherms studied including Langmuir, Freundlich, Temkin, Dubinin-Radushkevich, Flory Huggins, Fowler-Guggenheim, Hill-Deboer, Jovanovic, Harkin-Jura, and Halsey. In addition, this study studied the mechanism of renewable carbon adsorption from mangosteen peel. Most mangosteen is grown in Southeast Asia, particularly in Indonesia. The peel of the mangosteen fruit, which is typically discarded, contains lignin and hemicellulose molecules, which are the main building blocks for carbon. As a result, carbon made from mangosteen rind is ready for

use in wastewater treatment [30]. The current study highlights a sustainable approach to removing dyes from wastewater. In this study, curcumin was used as a model dye. Also, this study does not only focus on synthesis and characteristics but also evaluates the studied adsorption isotherm properties based on the use of various microparticle sizes (i.e. 500, 1000, and 2000 μm). Therefore, it is crucial for the advancement of wastewater decontamination utilizing sustainable and ecologically friendly adsorbents to provide an updated and focused review that summarizes the adsorption performance of effluent-derived adsorbents to remove dye effluents.

2. Theoretical Adsorption Isotherm

To understand the adsorption mechanism, ten adsorption isotherms were used and compared with the results of the fitting data. The calculation results to obtain the curve from the fitting data are shown in Table 1. In more detail, how to calculate the adsorption isotherm is described in the previous literature [31].

Table 1
Overview of ten adsorption isotherm models

Isotherm Model	Theoretical Explanation	Plot (x-axis vs y-axis)	Parameter
Langmuir	This model is used to describe the equilibrium between adsorbate and adsorbent system in which adsorbate adsorption is limited to one molecular layer at or before a relative pressure of unity is reached, supported using Eq. (1): $\frac{1}{Qe} = \frac{1}{Qmax^{Kl}}\frac{1}{C_e} + \frac{1}{Qmax}$ (1) where K_L is the Langmuir constant, *qe* is the number of molecules adsorbed at equilibrium (mg/g), and *qm* is the adsorption capacity (mg/g). Eq. (2) express the adsorption factor (R_L). $R_L = \frac{1}{1+ K_L C_e}$ (2) R_L describes favorable adsorption or no desorption ($0 < R_L < 1$); unfavorable adsorption ($R_L > 1$); linear adsorption (affected by the amount and concentration of adsorbed molecules) ($R_L = 1$); too strong adsorption or irreversible adsorption ($R_L = 0$).	$\frac{1}{C_e}$ vs $\frac{1}{Q_e}$	• $\frac{1}{Q_{max}} = intercept$ • $K_L = \frac{1}{Q_{max} \times slope}$
Freundlich	The surface heterogeneity and the exponential distribution of the functional sites are described by the Freundlich isotherm approximation. Freundlich isotherm adsorption is another term for multilayer adsorption. Freundlich isotherm represented by Eq. (3). $log\ Q_e = logk_f + \frac{1}{n} log\ \ C_e$ (3) where C_e is the adsorbate concentration at equilibrium (mg/L) and k_f is the Freundlich constant that estimates the adsorption capacity.	lnC_e vs lnQ_e	• $lnK_F = intercept$ • $\frac{1}{n} = slope$

	n is the degree of nonlinearity and the adsorption strength, following chemisorption ($n < 1$) or physisorption ($n > 1$); linear adsorption (a concentration-independent partition between two phases) ($n = 1$); normal adsorption ($1/n < 1$); cooperative adsorption ($1/n > 1$); favorable adsorption or no desorption ($1 < 1/n < 0$); and adsorption on a heterogeneous surface ($0 < 1/n < 1$; the closer to zero indicates increasing heterogeneous adsorbent surface).		
Temkin	This model assumes that the adsorption heat of all molecules decreases linearly with the increase in coverage of the adsorbent surface, and that adsorption is characterized by a uniform distribution of binding energies, up to a maximum binding energy, represented by Eq. (4). $q_e = B_T ln A_T + B_T ln C_e$ (4) where A_T is the equilibrium constant of the Temkin model. B_T is the Temkin constant, informing physical ($B_T < 8$ kJ) or chemical ($B_T > 8$ kJ) adsorption.	lnC_e vs Q_e	• $B = slope$ • $B_T ln A_T = intercept$ • $B_T = \frac{RT}{B}$
Dubinin-Radushkevich	This model assumes the adsorption of gases by porous adsorbents and the pore-filling mechanism, described by Eq. (5). $q_e = q_e \exp(-K_{DR\varepsilon^2})$ $\beta = K_{DR}$ (5) $lnq_e = lnq_s - (\beta\varepsilon^2)$ where q_s is the saturation capacity (mg/g) and β is the Dubinin-Radushkevich constant correlating to the average free adsorption energy. ε is the Polanyi potential associated with equilibrium conditions, in which the value correlates to adsorption energy (E) (see Eq. (6) and Eq. (7)): $\varepsilon = RTln\left[1 + \frac{1}{C_e}\right]$ (6) $E = \frac{1}{\sqrt{2\beta}}$ (7) E relates to the physical ($E < 8$ kJ) or chemical ($E > 8$ kJ) adsorption.	ε^2 *vs* lnQ_e	• $\beta = K_{DR} = slope$ • $E = \frac{1}{\sqrt{2\times K_{DR}}}$
Flory-Huggins	This model is used to explain how the adsorbent contacts and interacts with the adsorbate in the multilayer adsorption, represented in Eq. (8). $log\ \frac{\theta}{Ce} = log\ log\ K_{FH} + n_{FH}\ log\ log\ (1-\theta)$ (8) where $\theta = \left(1 - \frac{C_e}{C_o}\right)$ is the degree of monolayer coverage. n_{FH} and K_{FH} are the equilibrium constant for the Flory-Huggins model, in which it correlates to the Gibbs free energy ($\Delta G°$), as presented in Eq. (9):	$log\ \left(\frac{\theta}{C_0}\right)$ *vs* $log(1-\theta)$	• $n_{FH} = slope$ • $k_{FH} = intercept$ • $\Delta G^{o} = RTln(k_{FH})$ • $\theta = 1 - (\frac{C_e}{C_0})$

	$\Delta G° = -RT\ ln\ K_{FH}$ (9) when $\Delta G°$ is negative, it can describe the spontaneous and temperature-dependent nature of adsorption.		
Fowler-Guggenheim	This model considers lateral interaction of adsorbed species within a localized domain, with evidenced Van der Waals interactional effect between species adsorbed on neighboring sites, explicitly explained by Eq. (10). $ln\left[\frac{C_e(1-\theta)}{\theta}\right] = -lnK_{FG} + \frac{2W\theta}{RT}$ (10) where K_{FG} is the Fowler-Guggenheim constant (L/mg). W is the interaction energy between the adsorbed molecules (kJ/mol), informing processes under exothermic ($W > 0$), endothermic ($W < 0$ kJ/mol), or no interaction between adsorbed molecules ($W = 0$ kJ/mol).	θ vs $ln\left[\frac{C_e(1-\theta)}{\theta}\right]$	• $W = slope$ • $-lnK_{FG} = intercept$ • $\alpha\ (slope) = \frac{2W\theta}{RT}$ • $\theta = 1 - (\frac{C_e}{C_0})$
Hill Deboer	This model describes mobile with an allowance of lateral interaction between the molecules that have been adsorbed based on the values of the model's parameters, expressed in Eq. (11): $ln\left[\frac{C_e(1-\theta)}{\theta}\right] - \frac{\theta}{1-\theta} = -lnK_1 - \frac{K_2\theta}{RT}$ (11) where K_1 (L/mg) and K_2 (kJ/mol) are the contact energy constants for the adsorbed molecules, K_2 informing: exothermic with intermolecular adsorption ($K_2 > 0$); endothermic with repulsion ($K_2 < 0$), or no interaction between adsorbates ($K_2 = 0$).	θ vs $ln\left[\frac{C_e(1-\theta)}{\theta}\right] - \frac{\theta}{1-\theta}$	• $-lnk_1 = intercept$ • $\alpha\ (slope) = \frac{k_2\theta}{RT}$ • $\theta = 1 - (\frac{C_e}{C_0})$
Jovanovic	This model represents phenomena involving the elimination of mechanism interactions, similar to the Langmuir model (presented in Eq. (12)): $lnQ_e = lnQ_{max} - K_jC_e$ (12) where Q_e is the amount of adsorbate in the adsorbent at equilibrium (mg/g), Q_{max} is the maximum adsorption of the adsorbate, and K_J is the Jovanovic constant. At high concentration of adsorbate, the preceding equation becomes the Langmuir isotherm.	C_e vs lnQ_e	• $K_J = slope$ • $lnq_{max} = intercept$
Harkin-Jura	This model considers the heterogeneous pore distribution on the surface of the adsorbent which allows multilayer adsorption to occur, represented in Eq. (13): $\frac{1}{q_e^2} = \frac{B_{HJ}}{A_{HJ}} - \left(\frac{1}{A}\right) logC_e$ (13) B_{HJ} is related to the specific surface area of the adsorbent and A_{HJ} is the Harkin-Jura constant.	$logC_e$ vs $\frac{1}{q_e^2}$	• $A_H = \frac{1}{Slope}$ • $\frac{B_H}{A_H} = intercept$

Halsey	This model describes a multilayer adsorption system at a relatively long distance from the surface, similar to the Freundlich model. The Halsey model applies to multilayer adsorption and heterogeneous surfaces with non-uniformly distributed adsorption heats, represented in Eq. (14): $Q_e = \frac{1}{n_H} lnK_H - \left(\frac{1}{n_H}\right) lnC_e$ (14) where K_H and n_H are Halsey's constants.	lnC_e vs lnQ_e	• $\frac{1}{n} = slope$ • $\frac{1}{n} lnK_H = intercept$

3. Methodology

3.1 Preparation of Carbon Microparticles as Biosorbent

Several raw materials used in this study were mangosteen peel (*Garcinia mangostan*a; purchased from a local market in Karawang, Indonesia), pure water (purchased from Borma market in Bandung, Indonesia), and curcumin (obtained by extracting from a local market in Bandung, Indonesia). Figure 1 shows the flowchart diagram of the experimental procedure.

Synthesis of carbon particles from mangosteen peel waste was done through several steps. In the initial step, 150 g of mangosteen peel were cleaned and washed. Then, the mangosteen peel was naturally dried under the sun for 12 hours. In the next step, the mangosteen peel was carbonized using an electric oven in a room atmosphere for 5 hours at a constant temperature of 250°C. Furthermore, to obtain the particle size distribution, a sieving test was carried out (CV. Yayasan Bumi Publikasi Nusantara, Indonesia, hole variations of 2000, 1000, 500, 250, 125, 99, and 74 µm). In this study, particle sizes of 500, 1000, and 2000 µm were used for the adsorption experimental process.

3.2 Characterization of Carbon Microparticles as Biosorbent

To characterize the morphology and chemical structure of the carbon particle samples, Fourier Transform Infrared (FTIR-4600, Jasco Corp., Japan) and Digital Microscope (BXAW-AX-BC, China; magnification 1000x) were used.

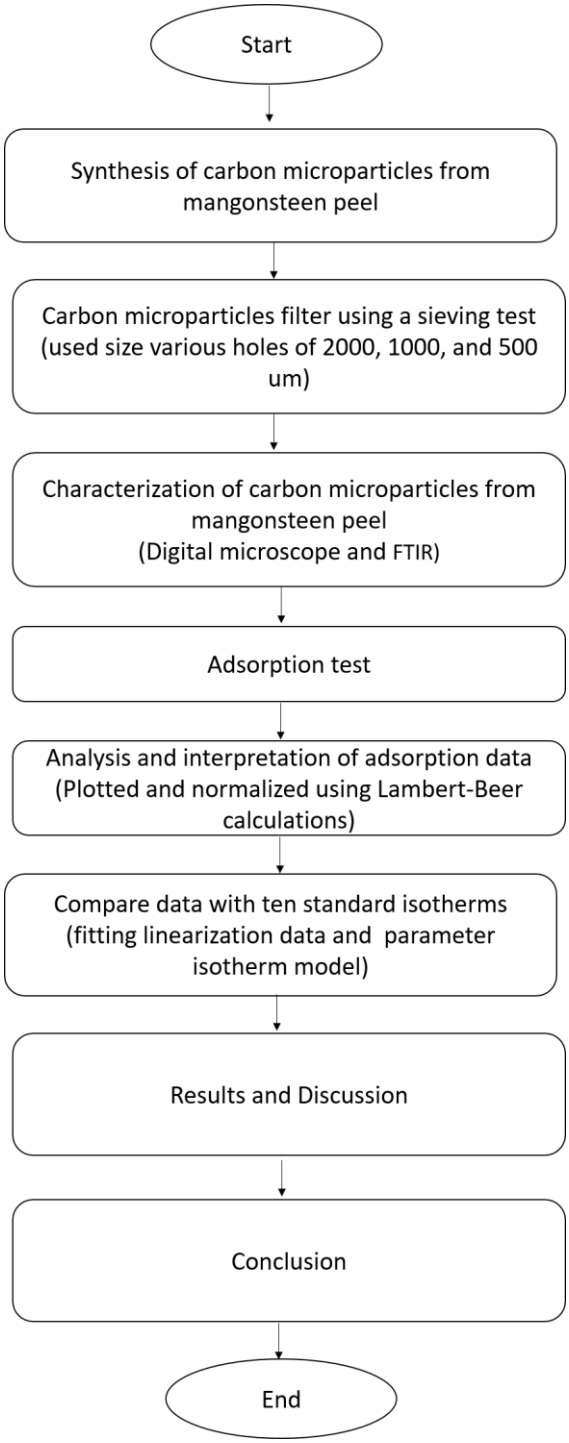

Fig. 1. Flowchart diagram of the experimental procedure

3.3 Adsorption Experimental Process

Before the adsorption process using curcumin as a dye model is carried out, several steps must be done first, including preparing a curcumin stock solution and preparing a calibration curve. In this study, a curcumin stock solution with a concentration of 100 ppm was prepared. The steps for preparing a curcumin stock solution were described in our previous study [32]. Preparation of the calibration curve was carried out by diluting the curcumin stock solution into a curcumin solution with a standard series solution of 20, 40, 60, 80, and 100 ppm. Then, the absorbance of curcumin

solutions with standard series solutions of 20, 40, 60, 80, and 100 ppm was measured at a wavelength of 250-500 nm using a UV-VIS instrument. The absorbance value obtained from the standard series solution produces a linear curve equation. Then, the concentration of the adsorbate (curcumin solution) adsorbed in the filtrate was calculated using the linear equation of the calibration curve that had been prepared. This absorbance value will depend on the concentration of the substance contained in the solution.

The next step is an adsorption experiment using curcumin solution as a dye model and using mangosteen peel-based carbon adsorbents. The adsorption test was carried out using the batch method. In short, the adsorption process was carried out by adding 0.5 g of prepared carbon particles (with sizes of 2000, 1000, and 500 µm) into a turmeric solution with a volume of 100 mL with various concentrations (20, 40, 60, 80, and 100 ppm). The turmeric solution was stirred manually for 1 hour. Then, the turmeric solution was decanted for 24 hours at room temperature and constant pH (about 7). Previously, blank solutions (turmeric solution without carbon) with various concentrations under the same conditions were tested as a comparison. During the adsorption process, a 3-mL aliquot of the sample solution was tested using a visible spectrophotometer (Model 7205 JENWAY; Cole-Parmer; US). The adsorption results were plotted and normalized using Lambert-Beer calculations. After that, the concentration data obtained were plotted and compared with standard isotherm adsorption models: Freundlich, Langmuir, Temkin, Dubinin-Radushkevich, Flory Huggins, Fowler-Guggenheim, Hill Deboer, Jovanovic, Harkin Jura, and Halsey.

4. Results

4.1 Characterization of Carbon Microparticles as Biosorbent

Figure 2(a) shows the results of the surface structure of carbon microparticles from mangosteen peel. In Figure 2(a), the physical form of carbon particles is black with irregular shapes. Figure 2(b) represents the results of ferret analysis of the particle size distribution of carbon from mangosteen peel. In general, the carbon particles used have a size between 200-500 µm with an average particle size of 600 µm. Figure 2(c) is the result of FTIR analysis of carbon particles from mangosteen peel. As shown in Figure 2(c), all particles have several identical wavelengths functional groups at wavelengths including hydroxyl groups (-OH) in 3400-3500 cm^{-1}, aliphatic C-H compounds in 2854-3859 cm^{-1}, carbonyl compounds (C=O) in 1617-1817 cm^{-1}, the C-H group stretches in 1300-1400 cm^{-1}, the vibrational stretching of C-O in 1023-1200 cm^{-1} [33-35]. In this study, the characterization was only FTIR. Characterization using X-ray diffraction (XRD), Brauer-Emmett-Teller (BET), scanning electron microscope (SEM), and thermogravimetric analysis (TGA) will be carried out in future research. Here, the results of FTIR analysis are used to determine the similarity of functional groups present in carbon microparticles of various sizes. In addition, the results of this similarity analysis can also confirm that the tool process used does not change the functional groups of the carbon microparticles. This is important to be able to ensure that similar functional groups are present in carbon microparticles to make it easier to understand the effect of particle size on the adsorption phenomenon [23].

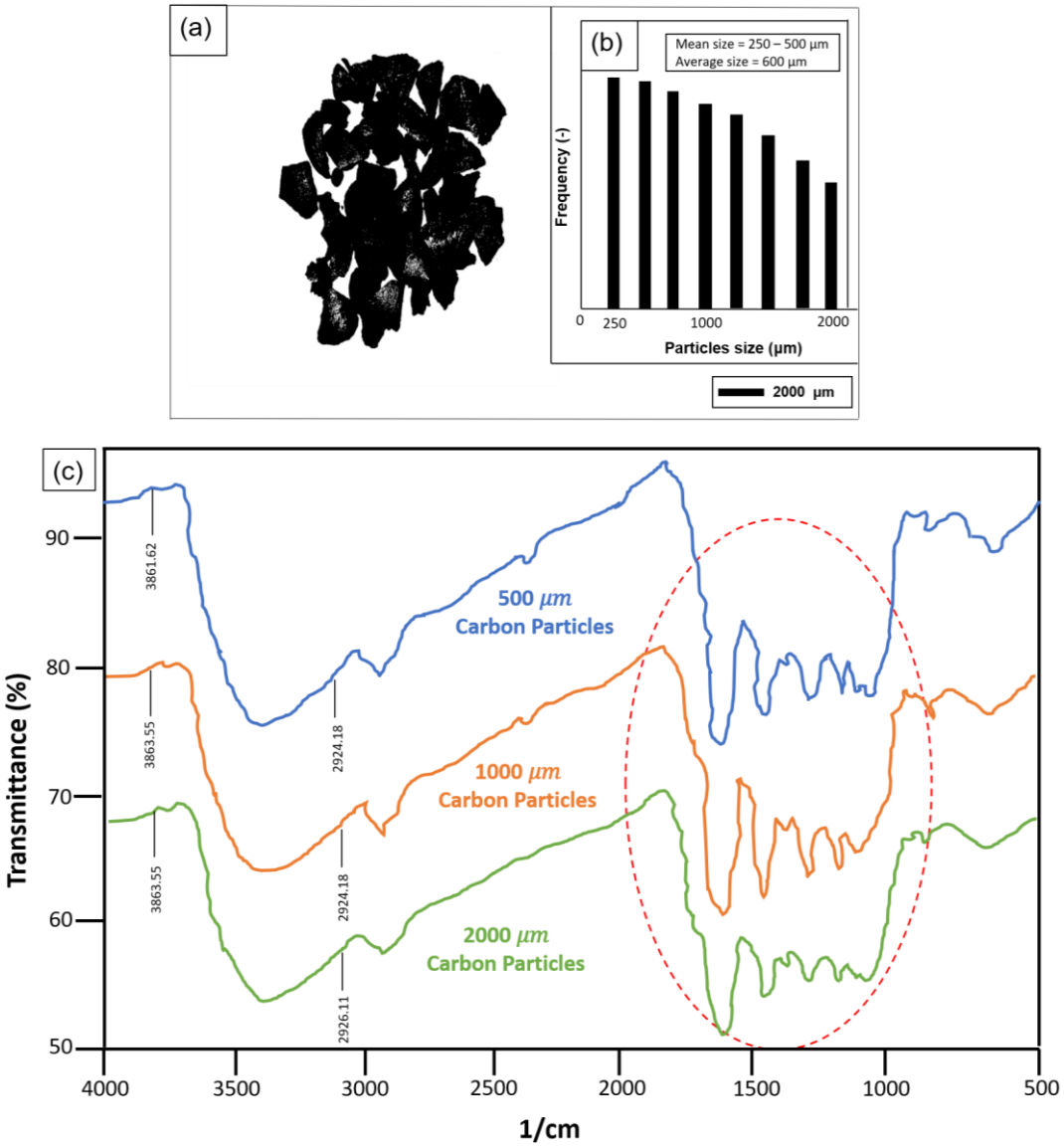

Fig. 2. Microscope images of carbon particles (a) with their size distribution (b). Figure (c) is the FTIR analysis results of carbon with different sizes

4.2 Adsorption Isotherm Model

Adsorption isotherm is one of the important studies in determining the adsorption equilibrium relationship quantitatively such as the characteristics of the pollutant that interacts with the adsorbent, optimizing the mechanism of the adsorption pathway, expressing surface properties, and adsorption capacity [36,37]. In this study, adsorption isotherms were evaluated by comparing the results of fitting the data with ten isotherm models (Langmuir, Freundlich, Temkin, Dubinin-Radushkevich, Flory Huggins, Fowler-Guggenheim, Hill-Deboer, Jovanovic, Harkin-Jura, and Halsey) based on various sizes particles (2000, 1000 and 500 µm).

To evaluate the adsorption isotherm model is assessed using the value of the correlation coefficient (R^2). The value of $R^2 > 0.80$ indicates that it is more suitable for the adsorption isotherm model. Figure 3(a) to Figure 3(j) represents the results of correlation plotting from adsorption isotherm analysis. Detailed calculation results for the ten isotherm models are presented in Table 2.

The Langmuir model assumes adsorption as homogeneous sites that transmigrate due to uniform energy [38]. The results of plotting the linearization of the Langmuir model are presented in Figure

3(a). Based on the correlation plot analysis of small-size carbon (500 µm) and large-size carbon (2000 and 1000 µm) fit with the Langmuir model because has an $R^2 > 0.80$. This informs that small-size and large-size carbon adsorption processes have the potential to form monolayer structures. The maximum capacity values (Q_{max}) of carbon measuring 500, 1000, and 2000 µm are 500,67; 333.33; and 244,45 mg/g, respectively (see Table 1). Based on the results of Q_{max} informs that the smaller carbon particle size increases the adsorption capacity. The R_L parameters show values in the range close to 0 which express the characteristics of carbon under favorable conditions for all adsorption systems [38]. The K_L parameter describes the interaction between the adsorption particles and the adsorbent. The small value of K_L indicates that the interaction between the adsorbate and the adsorbent is weak.

The Freundlich model views adsorption as a non-ideal that occurs on the multilayer surface with exponentially distributed energy [39]. Figure 3(b) is the result of fitting the Freundlich linearization model. Based on experiments, the value of R^2 for large-size carbon (1000 and 2000 µm) has a value greater than 0.80 and indicates suitable with the Freundlich model. This informs the formation of a multilayer surface system. In contrast, small-size carbon (500 µm) has an $R^2 < 0.80$ which shows the formation of a monolayer surface system. The parameter value of n_f is the intensity of adsorption that represents the process preference. Based on the value of n_f greater than 1 informing adsorption occurs in the physical system [39]. Analysis of $1/n_f$ value smaller than 0 informs the characteristics of carbon adsorption occurs favorable process.

The Temkin model describes the process of cooperative adsorption with the concentration of adsorbate considering the decrease in molecular heat absorption in the layer to decrease linearly [40]. Figure 3(c) depicts the results of the Temkin model correlation plotting. The correlation value for large-size carbon (1000 and 2000 µm) is suitable with the Temkin model ($R^2 > 0.80$) which shows the formation of a homogeneous system. However, the correlation value for small-size carbon (500 µm) has an $R^2 < 0.80$ which informs the formation of a heterogeneous system. The $\acute{o}_T$ parameter value is associated with the maximum energy bond that occurs in physical adsorption ($\acute{o}_T < 8$ kJ/mol).

The Dubinin-Radushkevich model describes a pore-filling process that can be applied to a range of media concentrations from multilayer adsorbates by considering the Gaussian free energy [41]. The parameter of *E* describes the adsorption process that occurs based on physical properties ($E < 8$ kJ/mol) and chemical adsorption (*E:* 8-16 kJ/mol) [42]. In this study the energy *E* for sizes 500, 1000, and 2000 is 0.582; 1.355; and 1.345 kJ/mol, respectively. This indicates that the physical adsorption process is more dominant in the operating system ($E < 8$ kJ/mol). Based on the correlation value (R^2) in Figure 3(d), R^2 is greater than 0.80 for large-size carbon, indicating filling the pore. Meanwhile, small-size carbon occurs in monolayer formation due to $R^2 < 0.80$.

According to the Flory-Huggins isotherm expressing the pore surface of the adsorbent [43]. In this case, the correlation value of R^2 is considered. Based on the correlation value, small-size carbon (size of 500 µm) has an R^2 value of less than 0.80 indicating the presence of a monolayer surface. Meanwhile, large-size carbon (1000 and 2000 µm) has an R^2 value greater than 0.80 indicating the presence of a multilayer surface (See Figure 3(e)). n_{FH} value represents the amount of adsorbent present in the adsorption zone. Large-size carbon has a lower n_{FH} value ($n_{FH} < 1$) that indicates the active zone of more than one adsorbent will be occupied by the adsorbate. In this model, Energy gibs are evaluated which indicates a non-spontaneous process ($\Delta G° > 0$) for small-size carbon. Meanwhile, Gibbs energy indicates a spontaneous process ($\Delta G° < 0$) for large-size carbon.

The Fowler-Guggenheim model assumes the lateral interactions of species that absorb the local dominance that exists between species [44]. The value of *W* represents the empirical interaction energy of the two species present near the site. Based on the experimental results, three particle sizes have *W* values less than 0 which indicates interactions that are not attractive between adsorbed

molecules. As a result, the loading increases due to the adsorption process' need for external energy, which reduces interaction. Figure 3(f) is an interpretation of the Fowler-Guggenheim linearization. Based on the R^2 value, small-size, and large-size carbon occurs in monolayer ($R^2 < 0.7$) and multilayer ($R^2 > 0.7$) formation, respectively.

The Hill-Deboer model expresses lateral interaction in adsorbing molecules [29]. Parameters K_1 and K_2 as Hill-de Boer constants and energy constants from the interaction effect between adsorbed sorbate molecules, respectively. A small K_2 value indicates weak lateral interactions, affinity, and attractions between adsorbed molecules. The results of fitting the Hill-Deboer correlation graph are represented in Figure 3(g). The small-size carbon (500 µm) has an $R^2 < 0.80$ that represents the monolayer formation. Meanwhile, the large-size carbon (2000 and 1000 µm) has a greater correlation value ($R^2 > 0.80$) which indicates a multilayer system.

Figure 3(h) is the fitting curve of the Jovanovic model linearization. The Jovanovic model has an $R^2 < 0.80$ for small-size carbon (500 µm) adsorption system and $R^2 > 0.80$ for large-size carbon (2000 and 1000 µm) adsorption system. Therefore, adsorption using small-size and large-size carbon follow multilayer and monolayer formation, respectively. The Jovanovic isotherm shows a good agreement with the Langmuir isotherm, in which particles with small sizes have the maximum adsorption capacity. The adsorption capacities for the 500, 1000, and 2000 nm were 1072.986; 257.516; and 28.598 mg/g, respectively.

The Harkin-Jura model considers the possibility of multilayer adsorption due to the heterogeneous surface distribution [44]. Figure 3(i) shows the linearization graph of the Harkin-Jura model. Based on the correlation value, small-size (500 µm) and large-size carbon (1000 and 2000 µm) have an R^2 greater than 0.80 indicating the presence of multilayer adsorption.

The Halsey model is used to evaluate multilayer adsorption systems [45]. Figure 3(j) depicts the plot of the results of the Halsey model analysis. Based on this model, large-size carbon (1000 and 2000 µm) has suitability as seen from the value of $R^2 > 0.80$ which indicates a multilayer system. Meanwhile, small-size carbon (500 µm) is not suitable because the correlation value is smaller than 0.80.

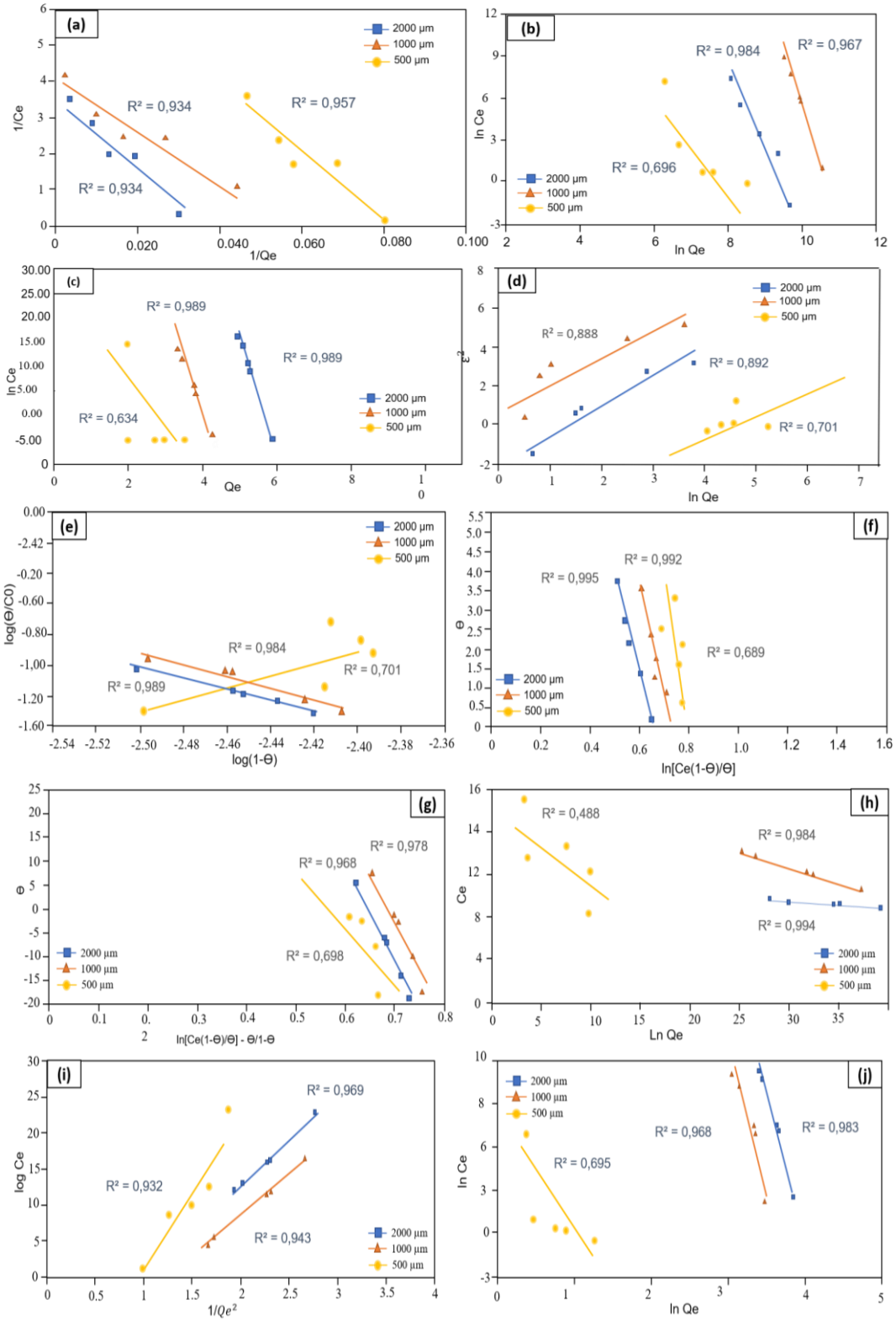

Fig. 3. Data fitting with isotherm models (a) Langmuir, (b) Freundlich, (c) Temkin, (d) Dubinin-Radushkevich, (e) Flory-Huggins, (f) Fowler-Guggenheim, (g) Hill-Deboer, (h) Jovanovic, (i) Harkin-Jura, and (j) Halsey

Table 2
Detailed data of adsorption isotherm parameters

Model	Parameter	Particle Size			Note
		500	1000	2000	
Langmuir	Q_{max} (mg/g)	500.670	333.330	244.450	The maximum adsorption capacity of the adsorbent
	K_L (L/mg)	1.047	-0.137	-0.133	The small value of the Langmuir constant demonstrates the weak interaction between adsorbate and adsorbent.
	R^2	0.957	0.934	0.934	• $R^2 > 0.8$ is a monolayer • $R^2 < 0.8$ is a multilayer
	R_L	1.8×10^{-5}	0.028	0.011	Favorable adsorption ($0 < 1/n < 1$)
Freundlich	K_F	1.768	1.462	1.268	The adsorption capacity of the adsorbent
	$1/n_f$	0.570	0.380	0.238	Close to 1, indicating favorable adsorption
	n_F	1.754	2.631	4.201	Higher than 1, physisorption
	R^2	0.696	0.967	0.984	• $R^2 > 0.8$ is a multilayer • $R^2 < 0.8$ is a monolayer
Temkin	β_T (J/mol)	0.400	-0.512	-0.123	Physisorption ($\beta_T < 8$ kJ/mol)
	A_T (L/g)	546.934	-738.674	-12824.205	The Temkin equilibrium binding constant
	R^2	0.634	0.989	0.989	• Homogenous adsorbate in the adsorbent surface ($R^2 > 0.80$) • Heterogenous adsorbate in the adsorbent surface ($R^2 < 0.80$)
Dubinin-Radushkevich	β (K_{DR})	1.474	0.272	0.276	The Dubinin-Radushkevich isotherm constant
	E (kJ/mol)	0.582	1.355	1.345	• Under 8, Physisorption
	R^2	0.701	0.888	0.892	• $R^2 > 0.8$ $is\ multilayer$ • $R^2 < 0.8$ $is\ monolayer$
Flory-Huggins	n_{FH}	5.910	-4.131	-2.131	Less than 1, the adsorbate fills more than one active adsorbent zone.
	K_{FH}	3.262×10^{13}	1.985×10^{-11}	1.585×10^{-11}	The Flory-Huggins isotherm constant
	$\Delta G°$	763.284	-604.486	-302.453	Higher than 0, a non-spontaneously adsorption
	R^2	0.701	0.984	0.989	• $R^2 < 0.8$ $is\ monolayer$ • $R^2 > 0.8$ $is\ multilayer$
Fowler-Guggenheim	K_{FG}	8.637×10^{-8}	9.257×10^{-6}	10.543×10^{-5}	The Fowler-Guggenheim isotherm constant
	W	17.810	-11.622	-8.564	Less than 0, a repulsive interaction between adsorbed molecules.
	R^2	0.689	0.992	0.995	• $R^2 > 0.8$ $is\ multilayer$ • $R^2 < 0.8$ $is\ monolayer$
Hill-Deboer	K_1	4.108	1.477×10^{-13}	0.523×10^{-8}	The Hill-Deboer isotherm constant
	K_2	4136.197	-1187.104	-2284.690	Less than 0, weak attraction between adsorbed molecules on a surface homogenous
	R^2	0.698	0.968	0.978	• $R^2 > 0.8$ $is\ multilayer$ • $R^2 < 0.8$ $is\ monolayer$
Jovanovic	K_J	-0.123	0.058	-0.005	The Jovanovic isotherm constant
	Q_{max}	1072.986	257.516	28.598	The maximum adsorption of adsorbate

	R^2	0.488	0.984	0.994	• $R^2 > 0.8$ *is monolayer* • $R^2 < 0.8$ *is multilayer*
Harkin-Jura	A_{HJ}	0.0262	16.067	86.338	The Harkin-Jura isotherm constant
	R^2	0.932	0.943	0.969	• $R^2 > 0.8$ *is multilayer* • $R^2 < 0.8$ *is monolayer*
Halsey	n_H	-0.261	-3.623	-4.200	The isotherm constant of Halsey
	K_H	0.119	0.119	0.119	The Halsey isotherm constants
	R^2	0.695	0.968	0.983	• $R^2 > 0.8$ *is multilayer* • $R^2 < 0.8$ *is monolayer*

In the previous explanation, a summary can be made regarding the suitability of the model for various sizes of carbon particles from mangosteen peel by looking at the results of fitting R^2 > 0.80, as follows

i. Small-size carbon (500 µm) has the order of best fit of the adsorption model: Langmuir > Harkin-Jura.
ii. Large-size carbon (1000 µm) has the order of best fit of the adsorption model: Hill-Deboer > Flory-Huggins > Fowler-Guggenheim.
iii. Large-size carbon (2000 µm) has the order of best fit of the adsorption model: Freundlich > Flory-Huggins > Fowler-Guggenheim.

Based on the results of the adsorption model suitability for various particle sizes, the adsorption mechanism can be explained. Details of the proposed adsorption mechanism based on the adsorption isotherm model are illustrated in Figures 4(a) and 4(b). During the adsorption process, when the carbon particles are small in size (500 µm), they form a monolayer system that is favorable for physisorption, filling the pores with many active sites, and repulsive interactions between the adsorbates. Meanwhile, the adsorption process of large particles (1000 and 2000 µm) studied is forming a multilayer system that is advantageous in terms of physisorption, pore filling of many active sites, and repulsive interactions between adsorbates. Formation of a monolayer that occurs without any interaction between adsorbed molecules and has the same energy on the surface (without any transmigration from the adsorbate). Meanwhile, multilayer adsorption occurs due to the heterogeneous distribution of energy in the active site of the adsorbent. Adsorption that occurs after the formation of monolayers and multilayers occurs due to the binding energy of the physisorption characteristics caused by the presence of Van der Waals forces, while geometric irregularities and energy inhomogeneity of the surface profile are the main causes for the formation of single layers [46]. In this study, the adsorption process requires external energy to take place properly. The formation of a monolayer on adsorption using small-sized carbon is caused by the small-sized carbon not providing enough active sites (such as the absence of a pore structure on the surface) for the adsorbate. Meanwhile, in large-sized carbon, the formation of multilayers is due to the presence of a pore-filling mechanism in the adsorbent surface. Based on the ten findings, the difference in particle size affects the maximum adsorption capacity. Small-size carbon has a larger maximum capacity value. Conversely, large carbon has a small maximum capacity value. This is because smaller particles have a larger surface area so they can provide more adsorption sites [47]. To confirm and prove that small-sized carbon particles have a larger q_{max} following the experiments, it is necessary to provide an adsorption equilibrium curve that measures the surface area of the adsorbent. Studies on adsorbent modification, leaching phenomena, lyophilic and lyophobic appearances, interfacial phenomena (roughness and contact angle), and comparative studies in the same field with other modified adsorbents were not carried out in this study. However, these studies will be carried out in future research.

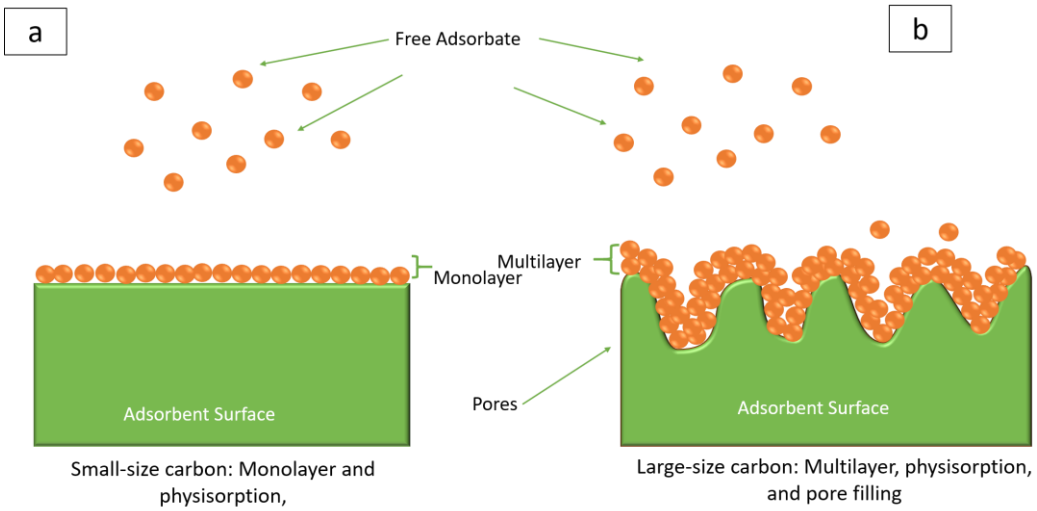

Fig. 4. Adsorption mechanism for particle size adsorbents of 500 (a) and 1000 and 2000 µm (b)

5. Conclusion

Carbon characteristics of mangosteen peel used to adsorb curcumin molecules (as an adsorbate model) have been successfully analyzed. Differences in particle size have been studied to find out the suitability of adsorption isotherm models and adsorption mechanisms. The isotherm model is suitable for small-size carbon (500 µm), such as Langmuir and Harkin-Jura. For the large-sized carbon with sizes of 1000 µm, the order of the suitable adsorption model is following Hill-Deboer, Flory-Huggins, and Fowler-Guggenheim, sequentially. For the large-sized carbon with sizes of 2000 µm, the order of the suitable adsorption model is Freundlich, Flory-Huggins, and Fowler-Guggenheim, sequentially. The mechanism of small carbon particles occurs in the adsorption process forming a monolayer surface mechanism. For large carbon particles, it forms a multilayer surface mechanism. During the adsorption process, the favorable physical adsorption process takes place non-spontaneously with pore filling and requires external energy. Small-sized carbon does not provide enough active sites (such as the absence of a pore structure on the surface) for the adsorbate, leading to the creation of monolayer adsorption during adsorption. In large-sized carbon, the pore-filling mechanism in the adsorbent surface cause multilayer development. This research is important to understand the application of adsorption by observing the phenomena that occur during the process.

Acknowledgment

This study was supported by Universitas Pendidikan Indonesia (Grant: Bangdos).

References

[1] Nandiyanto, Asep Bayu Dani, Ajeng Sukmafitri, Risti Ragadhita, Rosi Oktiani, Nuria Haristiani, and Ida Hamidah. "Conventional filter for the water treatment system in rural area." *Journal of Engineering Science and Technology* 14, no. 4 (2019): 2090-2097.

[2] Nandiyanto, A. B. D., and N. Haristiani. "Design of simple water treatment system for cleaning dirty water in the rural area." In *IOP Conference Series: Materials Science and Engineering*, vol. 180, no. 1, p. 012148. IOP Publishing, 2017. https://doi.org/10.1088/1757-899X/180/1/012148

[3] Joseph, Lesley, Byung-Moon Jun, Joseph RV Flora, Chang Min Park, and Yeomin Yoon. "Removal of heavy metals from water sources in the developing world using low-cost materials: A review." *Chemosphere* 229 (2019): 142-159. https://doi.org/10.1016/j.chemosphere.2019.04.198

[4] Xia, Jing, Yanxin Gao, and Gang Yu. "Tetracycline removal from aqueous solution using zirconium-based metal-organic frameworks (Zr-MOFs) with different pore size and topology: Adsorption isotherm, kinetic and mechanism studies." *Journal of Colloid and Interface Science* 590 (2021): 495-505. https://doi.org/10.1016/j.jcis.2021.01.046

[5] Akartasse, Noureddine, Khalil Azzaoui, Elmiloud Mejdoubi, Belkheir Hammouti, Lhaj Lahcen Elansari, Mohamed Abou-Salama, Mohamed Aaddouz, Rachid Sabbahi, Larbi Rhazi, and Mohamed Siaj. "Environmental-friendly adsorbent composite based on hydroxyapatite/hydroxypropyl methyl-cellulose for removal of cationic dyes from an aqueous solution." *Polymers* 14, no. 11 (2022): 2147. https://doi.org/10.3390/polym14112147

[6] de Souza, Renata Mariane, Daiana Seibert, Heloise Beatriz Quesada, Fátima de Jesus Bassetti, Márcia Regina Fagundes-Klen, and Rosângela Bergamasco. "Occurrence, impacts and general aspects of pesticides in surface water: A review." *Process Safety and Environmental Protection* 135 (2020): 22-37. https://doi.org/10.1016/j.psep.2019.12.035

[7] Lima, Eder C. "Removal of emerging contaminants from the environment by adsorption." *Ecotoxicology and Environmental Safety* 150 (2018): 1-17. https://doi.org/10.1016/j.ecoenv.2017.12.026

[8] Zhang, Xiaoyuan, Ping Gu, and Yu Liu. "Decontamination of radioactive wastewater: State of the art and challenges forward." *Chemosphere* 215 (2019): 543-553. https://doi.org/10.1016/j.chemosphere.2018.10.029

[9] Ahmaruzzaman, Md. "Adsorption of phenolic compounds on low-cost adsorbents: a review." *Advances in Colloid and Interface Science* 143, no. 1-2 (2008): 48-67. https://doi.org/10.1016/j.cis.2008.07.002

[10] Jodeh, S., N. Basalat, A. Abu Obaid, D. Bouknana, B. Hammouti, T. B. Hadda, W. Jodeh, and I. Warad. "Adsorption of some organic phenolic compounds using activated carbon from cypress products." *Journal of Chemical and Pharmaceutical Research* 6, no. 2 (2014): 713-723.

[11] Al-Gheethi, Adel Ali, Qasdina Marsya Azhar, Ponnusamy Senthil Kumar, Abdiadim Abdirizak Yusuf, Abdullah Khaled Al-Buriahi, Radin Maya Saphira Radin Mohamed, and Muhanna Mohammed Al-Shaibani. "Sustainable approaches for removing Rhodamine B dye using agricultural waste adsorbents: A review." *Chemosphere* 287 (2022): 132080. https://doi.org/10.1016/j.chemosphere.2021.132080

[12] Holkar, Chandrakant R., Ananda J. Jadhav, Dipak V. Pinjari, Naresh M. Mahamuni, and Aniruddha B. Pandit. "A critical review on textile wastewater treatments: possible approaches." *Journal of Environmental Management* 182 (2016): 351-366. https://doi.org/10.1016/j.jenvman.2016.07.090

[13] Karimi-Maleh, Hassan, Sara Ranjbari, Bahareh Tanhaei, Ali Ayati, Yasin Orooji, Marzieh Alizadeh, Fatemeh Karimi et al. "Novel 1-butyl-3-methylimidazolium bromide impregnated chitosan hydrogel beads nanostructure as an efficient nanobio-adsorbent for cationic dye removal: Kinetic study." *Environmental Research* 195 (2021): 110809. https://doi.org/10.1016/j.envres.2021.110809

[14] Manavi, Narges, Amir Sadegh Kazemi, and Babak Bonakdarpour. "The development of aerobic granules from conventional activated sludge under anaerobic-aerobic cycles and their adaptation for treatment of dyeing wastewater." *Chemical Engineering Journal* 312 (2017): 375-384. https://doi.org/10.1016/j.cej.2016.11.155

[15] Bayomie, Omar S., Haitham Kandeel, Tamer Shoeib, Hu Yang, Noha Youssef, and Mayyada MH El-Sayed. "Novel approach for effective removal of methylene blue dye from water using fava bean peel waste." *Scientific Reports* 10, no. 1 (2020): 7824. https://doi.org/10.1038/s41598-020-64727-5

[16] Noman, Efaq, A. A. Al-Gheethi, Balkis A. Talip, Radin Mohamed, and Amir Hashim Kassim. "Oxidative enzymes from newly local strain Aspergillus iizukae EAN605 using pumpkin peels as a production substrate: Optimized production, characterization, application and techno-economic analysis." *Journal of Hazardous Materials* 386 (2020): 121954. https://doi.org/10.1016/j.jhazmat.2019.121954

[17] Rusin, Casey J., Mounir El Bakkari, Rongbing Du, Yaman Boluk, and Mark T. McDermott. "Plasmonic cellulose nanofibers as water-dispersible surface-enhanced Raman scattering substrates." *ACS Applied Nano Materials* 3, no. 7 (2020): 6584-6597. https://doi.org/10.1021/acsanm.0c01045

[18] Vieira, Wedja Timóteo, Marina Barbosa de Farias, Marcela Pires Spaolonzi, Meuris Gurgel Carlos da Silva, and Melissa Gurgel Adeodato Vieira. "Removal of endocrine disruptors in waters by adsorption, membrane filtration and biodegradation. A review." *Environmental Chemistry Letters* 18, no. 4 (2020): 1113-1143. https://doi.org/10.1007/s10311-020-01000-1

[19] Ragadhita, R. I. S. T. I., and ASEP BAYU DANI Nandiyanto. "Curcumin adsorption on zinc imidazole framework-8 particles: Isotherm adsorption using Langmuir, Freundlich, Temkin, and Dubinin-Radushkevich models." *Journal of Engineering Science and Technology* 17, no. 2 (2022): 1078-1089.

[20] Leal Filho, Walter, Fernanda Frankenberger, Amanda Lange Salvia, Ulisses Azeiteiro, Fatima Alves, Paula Castro, Markus Will et al. "A framework for the implementation of the Sustainable Development Goals in university programmes." *Journal of Cleaner Production* 299 (2021): 126915. https://doi.org/10.1016/j.jclepro.2021.126915

[21] Caineng, Z. O. U., Bo Xiong, X. U. E. Huaqing, Dewen Zheng, G. E. Zhixin, W. A. N. G. Ying, Luyang Jiang, P. A. N. Songqi, and W. U. Songtao. "The role of new energy in carbon neutral." *Petroleum Exploration and Development* 48, no. 2 (2021): 480-491. https://doi.org/10.1016/S1876-3804(21)60039-3

[22] Fang, N., K. Otsuka, A. Ishii, T. Taniguchi, K. Watanabe, K. Nagashio, and Y. K. Kato. "Hexagonal boron nitride as an ideal substrate for carbon nanotube photonics." *ACS Photonics* 7, no. 7 (2020): 1773-1779. https://doi.org/10.1021/acsphotonics.0c00406
[23] Fiandini, Meli, Risti Ragadhita, Asep Bayu Dani Nandiyanto, and Willy Cahya Nugraha. "Adsorption characteristics of submicron porous carbon particles prepared from rice husk." *Journal of Engineering Science and Technology* 15 (2020): 022-031.
[24] Nandiyanto, Asep Bayu Dani, Rina Maryanti, Meli Fiandini, Risti Ragadhita, Dian Usdiyana, Sri Anggraeni, Wafa Raihana Arwa, and Abdulkareem Sh Mahdi Al-Obaidi. "Synthesis of carbon microparticles from red dragon fruit (Hylocereus undatus) peel waste and their adsorption isotherm characteristics." *Molekul* 15, no. 3 (2020): 199-209. https://doi.org/10.20884/1.jm.2020.15.3.657
[25] Nandiyanto, Asep Bayu Dani, Gabriela Chelvina Santiuly Girsang, Rina Maryanti, Risti Ragadhita, Sri Anggraeni, Fajar Miraz Fauzi, Putri Sakinah et al. "Isotherm adsorption characteristics of carbon microparticles prepared from pineapple peel waste." *Communications in Science and Technology* 5, no. 1 (2020): 31-39. https://doi.org/10.21924/cst.5.1.2020.176
[26] Nandiyanto, Asep Bayu Dani. "Isotherm adsorption of carbon microparticles prepared from pumpkin (Cucurbita maxima) seeds using two-parameter monolayer adsorption models and equations." *Moroccan Journal of Chemistry* 8, no. 3 (2020): 745-761.
[27] Prieto-García, Francisco, Roberto A. Canales-Flores, Judith Prieo-Méndez, Otilio A. Acevedo-Sandoval, and Elena M. Otazo-Sánchez. "Evaluation of three lignocellulose biomass materials (barley husk, corn cobs, agave leaves) as precursors of activated carbon." *Revista de la Facultad de Ciencias* 11, no. 1 (2022): 17-39. https://doi.org/10.15446/rev.fac.cienc.v11n1.97719
[28] Ragadhita, R., A. Amalliya, S. Nuryani, M. Fiandini, A. B. D. Nandiyanto, A. Hufad, A. Mudzakir et al. "Sustainable Carbon-Based Biosorbent Particles from Papaya Seed Waste: Preparation and Adsorption isotherm." *Moroccan Journal of Chemistry* 11, no. 2 (2023): 395-410.
[29] Nayagam, J. Oliver Paul, and K. Prasanna. "Utilization of shell-based agricultural waste adsorbents for removing dyes: A review." *Chemosphere* 291 (2022): 132737. https://doi.org/10.1016/j.chemosphere.2021.132737
[30] Tran, Quoc Toan, Tra Huong Do, Xuan Linh Ha, Huyen Phuong Nguyen, Anh Tien Nguyen, Thi Cam Quyen Ngo, and Hung Dung Chau. "Study of the Ciprofloxacin Adsorption of Activated Carbon Prepared from Mangosteen Peel." *Applied Sciences* 12, no. 17 (2022): 8770. https://doi.org/10.3390/app12178770
[31] Ragadhita, Risti, and Asep Bayu Dani Nandiyanto. "How to calculate adsorption isotherms of particles using two-parameter monolayer adsorption models and equations." *Indonesian Journal of Science and Technology* 6, no. 1 (2021): 205-234. https://doi.org/10.17509/ijost.v6i1.32354
[32] Nandiyanto, A. B. D., A. S. Wiryani, A. Rusli, A. Purnamasari, A. G. Abdullah, I. Widiaty, and R. Hurriyati. "Extraction of curcumin pigment from Indonesian local turmeric with its infrared spectra and thermal decomposition properties." In *IOP Conference Series: Materials Science and Engineering*, vol. 180, no. 1, p. 012136. IOP Publishing, 2017. https://doi.org/10.1088/1757-899X/180/1/012136
[33] Nandiyanto, Asep Bayu Dani, Rosi Oktiani, and Risti Ragadhita. "How to read and interpret FTIR spectroscope of organic material." *Indonesian Journal of Science and Technology* 4, no. 1 (2019): 97-118. https://doi.org/10.17509/ijost.v4i1.15806
[34] Wathoni, Nasrul, Chu Yuan Shan, Wong Yi Shan, Tina Rostinawati, Raden Bayu Indradi, Rimadani Pratiwi, and Muchtaridi Muchtaridi. "Characterization and antioxidant activity of pectin from Indonesian mangosteen (Garcinia mangostana L.) rind." *Heliyon* 5, no. 8 (2019): e02299. https://doi.org/10.1016/j.heliyon.2019.e02299
[35] Tejamukti, Endjang Prebawa, Widiastuti Setyaningsih, Budiman Yasir, Gemini Alam, and Abdul Rohman. "Application of FTIR spectroscopy and HPLC combined with multivariate calibration for analysis of xanthones in mangosteen extracts." *Scientia Pharmaceutica* 88, no. 3 (2020): 35. https://doi.org/10.3390/scipharm88030035
[36] Lima, Eder C., Ahmad Hosseini-Bandegharaei, Juan Carlos Moreno-Piraján, and Ioannis Anastopoulos. "A critical review of the estimation of the thermodynamic parameters on adsorption equilibria. Wrong use of equilibrium constant in the Van't Hoof equation for calculation of thermodynamic parameters of adsorption." *Journal of Molecular Liquids* 273 (2019): 425-434. https://doi.org/10.1016/j.molliq.2018.10.048
[37] Al-Yousef, Haifa A., Badriah M. Alotaibi, Fatma Aouaini, Lotfi Sellaoui, and Adrian Bonilla-Petriciolet. "Adsorption of ibuprofen on cocoa shell biomass-based adsorbents: Interpretation of the adsorption equilibrium via statistical physics theory." *Journal of Molecular Liquids* 331 (2021): 115697. https://doi.org/10.1016/j.molliq.2021.115697
[38] Delgado, Nasly, Alberto Capparelli, Agustín Navarro, and Damián Marino. "Pharmaceutical emerging pollutants removal from water using powdered activated carbon: study of kinetics and adsorption equilibrium." *Journal of Environmental Management* 236 (2019): 301-308. https://doi.org/10.1016/j.jenvman.2019.01.116

[39] Walsh, Kenneth, Sebastian Mayer, Dirk Rehmann, Thomas Hofmann, and Karl Glas. "Equilibrium data and its analysis with the Freundlich model in the adsorption of arsenic (V) on granular ferric hydroxide." *Separation and Purification Technology* 243 (2020): 116704. https://doi.org/10.1016/j.seppur.2020.116704

[40] Karim, Kamal Hama. "Copper adsorption behavior in some calcareous soils using Langmuir, Freundlich, Temkin, and Dubinin-Radushkevich models." *Journal of Soil Sciences and Agricultural Engineering* 11, no. 1 (2020): 27-34. https://doi.org/10.21608/jssae.2020.79168

[41] Barbero, G., L. R. Evangelista, and I. Lelidis. "Effective adsorption energy and generalization of the Frumkin-Fowler-Guggenheim isotherm." *Journal of Molecular Liquids* 327 (2021): 114795. https://doi.org/10.1016/j.molliq.2020.114795

[42] Dada, Adewumi O., J. O. Ojediran, Abiodun A. Okunola, F. E. Dada, A. I. Lawal, A. P. Olalekan, and O. Dada. "Modeling of biosorption of Pb (II) and Zn (II) ions onto PaMRH: Langmuir, Freundlich, Temkin, Dubinin-Raduskevich, Jovanovic, Flory-Huggins, Fowler-Guggenheim and Kiselev comparative isotherm studies." *International Journal of Mechanical Engineering and Technology (IJMET)* 10, no. 2 (2019): 1048-1058.

[43] Safronov, A. P., L. V. Adamova, and G. V. Kurlyandskaya. "Flory-huggins parameters of guar gum, xanthan gum, agarose, and gellan gum in aqueous solutions." *Polymer Science, Series A* 61 (2019): 29-38. https://doi.org/10.1134/S0965545X19010139

[44] Pennanen, Toni, Varsha Srivastava, Mika Sillanpää, and Tuomo Sainio. "Compost: Potent biosorbent for the removal of heavy metals from industrial and landfill stormwater." *Journal of Cleaner Production* 273 (2020): 122736. https://doi.org/10.1016/j.jclepro.2020.122736

[45] Korkut, Fulya, and Didem Saloglu. "Synthesis, characterization, and tetracycline adsorption behavior of activated carbon dopped alginate beads: isotherms, kinetics, thermodynamic, and adsorption mechanism." *Desalination and Water Treatment* 206 (2020): 315-330. https://doi.org/10.5004/dwt.2020.26305

[46] Syafiuddin, Achmad, Mohamad Ali Fulazzaky, Salmiati Salmiati, Ahmad Beng Hong Kueh, Mohammad Fulazzaky, and Mohd Razman Salim. "Silver nanoparticles adsorption by the synthetic and natural adsorbent materials: an exclusive review." *Nanotechnology for Environmental Engineering* 5 (2020): 1-18. https://doi.org/10.1007/s41204-019-0065-3

[47] Ohlwein, Simone, Ron Kappeler, Meltem Kutlar Joss, Nino Künzli, and Barbara Hoffmann. "Health effects of ultrafine particles: a systematic literature review update of epidemiological evidence." *International Journal of Public Health* 64 (2019): 547-559. https://doi.org/10.1007/s00038-019-01202-7